

ESTIMATION OF THE REGULARIZATION PARAMETER IN LINEAR DISCRETE ILL-POSED PROBLEMS USING THE PICARD PARAMETER *

EITAN LEVIN[†] AND ALEXANDER Y. MELTZER[†]

Abstract. We present a new approach for determining the regularization parameter for general-form Tikhonov regularization of linear ill-posed problems. In our approach the regularization parameter is found by approximately minimizing the distance between the unknown noiseless data and the data reconstructed from the regularized solution. We obtain the approximation of this distance by employing the Picard parameter to separate the noise from the data in the coordinate system of the generalized SVD. The Picard parameter is found using a simple and reliable algorithm based on successive estimations of the noise variance from the Fourier coefficients of the data. Numerical examples demonstrate the accuracy and efficiency of our method¹.

Key words. ill-posed problem, inverse problem, generalized SVD, Picard parameter, Tikhonov regularization, regularization parameter

AMS subject classifications. 65R30, 65R32, 65F22

1. Introduction. The Tikhonov regularization method [33] is one of the most widely applied methods for solving linear ill-posed problem. It is well known that the accuracy of the solution obtained using this method depends crucially on the chosen regularization parameter. The regularization parameter is often obtained using the Generalized Cross-Validation (GCV) [37, 10], L-curve [14, 20], Quasi-optimality [1, 2], Stein's Unbiased Risk Estimate (SURE) [31, 29] or other methods. However, none of the above-mentioned methods find the regularization parameter in a consistent and robust manner. In particular, for a rank-deficient A or a singular L , the above-mentioned methods tend to produce solutions that significantly differ from the actual solutions in a non-negligible percentage of cases.

We can state the problem formally as follows. Given an ill-conditioned matrix A and vector b contaminated by noise, we solve the linear system

$$Ax = b. \quad (1.1)$$

Linear discrete ill-posed problems of the form (1.1) often arise from the discretization of Fredholm integral equations of the first kind [22, 11, 5, 34, 15], in image deblurring problems [19, 7, 40, 4, 26] and in machine learning algorithms [3, 35, 30, 41, 39]. The method of Tikhonov regularization replaces the original ill-posed problem (1.1) with a minimization problem

$$\min_x \{ \|Ax - b\|^2 + \lambda^2 \|Lx\|^2 \}, \quad (1.2)$$

where $\|\cdot\|$ is the ℓ^2 -norm, L is a regularization matrix and $\lambda \geq 0$ is a regularization parameter. The problem (1.2) is said to be in standard form if $L = I$, and in general form if $L \neq I$ [21, 12, 9]. The

*This research was supported by the Israel Science Foundation (grant No. 132/14).

[†]Department of Condensed Matter Physics, Weizmann Institute of Science, 76100 Rehovot, Israel (eitan.levin@weizmann.ac.il, alexander.meltzer@weizmann.ac.il).

¹ A MATLAB-based implementation of the proposed algorithms can be found at <https://www.weizmann.ac.il/condmat/superc/software/>

development of an accurate and reliable method for determination of the regularization parameter λ is the main subject of this paper.

The present work is closely related to that of O’Leary [25] and Taroudaki and O’Leary [32], who suggest a method for near-optimal estimation of the regularization parameter. The essence of this method is to determine the regularization parameter by approximate minimization of the mean-square error (MSE)

$$\text{MSE}(\lambda) \equiv \|x_{true} - x_\lambda\|^2, \quad (1.3)$$

where x_{true} is a solution of $Ax = b_{true}$, b_{true} is the unperturbed data vector and x_λ is the regularized solution of (1.2). The minimization is performed in the coordinate system of the SVD of A for the special case of $L = I$ by employing the Picard parameter. By definition, the Picard parameter corresponds to the index above which the Fourier coefficients, with respect to the left singular vectors of A of the perturbed data, are dominated by noise. Using the Picard parameter, the SVD expansion of the MSE can be split into two parts, the part containing the information about the unperturbed data, and the other part containing the noise. The first part can be replaced with its expected value, while the second part can be rewritten in terms of the known Fourier coefficients of the data. This sum splitting enables an accurate approximation of the MSE because the Fourier coefficients capture a large part of the true, oscillatory behavior around zero of the coefficients in the expansion of (1.3). The Picard parameter is estimated in [32] either manually, as the index where the plot of the Fourier coefficients of the data levels off, or, if the noise is Gaussian, by the Lilliefors test, as we explain in subsection 3.2.

Even though the method developed in [32, 25] gives accurate results in a large percentage of cases and is shown to compete favorably with some standard methods, it has several limitations that likely prevent it from becoming more broadly accepted. First, the method in [32, 25] does not allow the use of $L \neq I$ which is necessary in many applications in order to incorporate different desirable properties in the solution [6, 13, 21, 12]. In particular, L is often chosen to be the discrete approximation of a derivative operator to control various degrees of smoothness of the solution. The second, and even more important limitation is that the method is inaccurate for some noise realizations because the large variance of the Fourier coefficients precludes accurate estimation of the Picard parameter.

In this paper we strive to overcome the above limitations. To handle the case $L \neq I$, we replace the SVD of A used in [32, 25] with the generalized singular value decomposition (GSVD) of the pair (A, L) [27, 17]. It is significantly more difficult, however, to minimize the MSE (1.3) in the GSVD basis [32, sect. 2]. For this reason, we replace the MSE with the norm

$$f(\lambda) \equiv \|b - n - Ax_\lambda\|^2, \quad (1.4)$$

where n is the noise vector and $b - n = b_{true}$. The norm (1.4) has a simple GSVD expansion and approximately the same minimizer as the MSE. This is due to norm (1.4) having the same minimizer as the more familiar predictive mean-square error (PMSE)

$$\text{PMSE}(\lambda) \equiv \|Ax_{true} - Ax_\lambda\|^2, \quad (1.5)$$

which in turn is typically close to the minimizer of the MSE [24, 8] and under certain assumptions is identical to it [38]. To determine λ , we write norm (1.4) in terms of the GSVD of (A, L) under

very relaxed assumptions about the sizes and ranks of the matrices involved in (1.2). We give upper and lower bounds on the Picard parameter and employ them to efficiently estimate its value. Once the Picard parameter is found, we approximate the noise-dependent terms in the GSVD expansion of (1.4) by sum splitting similarly to [32, 25]. We call the resulting approximate minimization of (1.4) the Series Splitting (SS) method.

Approximate minimization of (1.4) can be alternatively performed using a more general two-step approach. Particularly, we can obtain an approximation $\hat{b} \approx b - n$ by applying an accurate filter based on the Picard parameter to b , substitute \hat{b} for $b - n$ in (1.4) and minimize the resulting norm $\|\hat{b} - Ax_\lambda\|^2$. The filter employs the Picard parameter to drop the noise-dominated components of the data in the coordinate system of the GSVD. The advantage of this approach is that it is independent of the chosen regularization method. It requires only a data filter and an algorithm for calculating the regularized solution given a regularization parameter. We call this method the Data Filtering (DF) approach.

The accuracy of the Picard parameter estimation algorithm [32] can be significantly improved by a simple modification. Specifically, we suggest to test the sequence of the Fourier coefficients in reverse order to that proposed in [32] and at a higher confidence level. We can also improve the performance of the algorithm by making use of upper and lower bounds on the Picard parameter to limit the number of required tests. However, in spite of the improvement in accuracy, the algorithm remains prone to errors because of the reliance on noisy series of Fourier coefficients. To avoid the dependence on noisy sequences altogether, we go a step further and propose a new method that relies on averages of the squared moduli of the Fourier coefficients. We prove that the sequence of these averages decreases with increasing index of the Fourier coefficients until it converges to the value of the noise variance at the Picard parameter. As a result, both the noise variance and Picard parameter can be estimated reliably by detecting the levelling off of the above sequence of averages.

The SS method is closely related to the SURE and GCV methods, both of which approximately minimize (1.4). Contrary to the SS and DF methods, the GCV and SURE do not split the sum in the GSVD expansion of (1.4). Moreover, we show that they both rely on replacing the whole sum in the expansion of (1.4) with its expected value, which results in a less accurate approximation to the true value of the expansion than could be achieved using the SS and DF methods. We give a detailed comparison of the methods in a series of numerical examples.

The structure of this paper is as follows. In section 2 we formulate the problem of Tikhonov regularization and solve it using the generalized singular value decomposition (GSVD). In section 3, we develop the SS and DF methods to approximately minimize the norm (1.4) and the algorithms for estimation of the Picard parameter. In section 4, we discuss the SURE and GCV methods. Finally, in section 5 we present the results of the numerical calculations.

2. Formulation of the problem. We solve the linear ill-posed problem (1.1) by the Tikhonov regularization using a general regularization matrix L . Throughout the paper, we make the following assumptions:

1. The problem (1.2) has a unique solution for any λ . This implies $\mathcal{N}(A) \cap \mathcal{N}(L) = \{0\}$ where $\mathcal{N}(\cdot)$ denotes the null-space of a matrix (see [17, sect. 5.1.1]).
2. The nullspace of L is spanned by smooth vectors. This assumption holds in most practical cases and is necessary to ensure proper filtering of the noise by the regularization, see [18, sect. 8.1], [17, sect. 2.1.2], [12, sect. 3].

3. The data vector b is perturbed by an additive noise whose components are independent random variables taken from a distribution with zero mean and constant variance s^2 .
4. The generalized singular values of (A, L) decay to zero with no significant gap. The smallest generalized singular values cluster at (machine) zero. This property is common for discrete ill-posed problems - see [17, sect. 2.1.2].
5. The problem satisfies the discrete Picard condition [13].

The Tikhonov minimization problem (1.2) is equivalent to the normal equation

$$(A^*A + \lambda^2 L^*L)x = A^*b, \quad (2.1)$$

thereby yielding the Tikhonov solution as

$$x_\lambda = (A^*A + \lambda^2 L^*L)^{-1} A^*b. \quad (2.2)$$

We rewrite (2.2) using the GSVD [27] of the pair (A, L) . Let $M^{m \times n}$ be the space of $m \times n$ matrices, $A \in M^{m \times n}$, and $L \in M^{p \times n}$. It follows from assumption 1 that $n = \text{rank}([A^T \ L^T])$ and therefore, $m + p \geq n$ (see [36, sect. 1]). Under these definitions the matrices A and L can be decomposed as

$$A = U \begin{pmatrix} I_A & & \\ & S_A & \\ & & O_A \end{pmatrix} Y^{-1}, \quad L = V \begin{pmatrix} O_L & & \\ & S_L & \\ & & I_L \end{pmatrix} Y^{-1}, \quad (2.3)$$

where $U \in M^{m \times m}$, $V \in M^{p \times p}$ are unitary, $Y \in M^{n \times n}$ is invertible, $S_A = \text{diag}\{\sigma_{r+1}, \sigma_{r+2}, \dots, \sigma_{r+q}\}$ and $S_L = \text{diag}\{\mu_{r+1}, \mu_{r+2}, \dots, \mu_{r+q}\}$ are real matrices, $O_A \in M^{(m-r-q) \times (n-r-q)}$, $O_L \in M^{(p+r-n) \times r}$ are zero matrices, and I_A and I_L are $r \times r$ and $(n-r-q) \times (n-r-q)$ identity matrices, respectively. The zero and identity matrices can be empty. The values $\{\sigma_k\}_{r+1}^{r+q}$ are arranged in decreasing order and $\{\mu_k\}_{r+1}^{r+q}$ in increasing order so that

$$1 > \sigma_{r+1} \geq \sigma_{r+2} \geq \dots \geq \sigma_{r+q} > 0, \quad 0 < \mu_{r+1} \leq \mu_{r+2} \leq \dots \leq \mu_{r+q} < 1. \quad (2.4)$$

In addition, the pairs satisfy the identity

$$\sigma_k^2 + \mu_k^2 = 1 \iff S_A^T S_A + S_L^T S_L = I_{q \times q}. \quad (2.5)$$

The quantities $\gamma_k = \sigma_k / \mu_k$ are called the generalized singular values of the pair (A, L) . Because of the ordering defined in (2.4), the sequence $\{\gamma_k\}_{r+1}^{r+q}$ is arranged in decreasing order.

To relate the parameters r and q to the ranks of A and L , we observe that

$$A^*A = (Y^{-1})^* D_A Y^{-1}, \quad L^*L = (Y^{-1})^* D_L Y^{-1}, \quad (2.6)$$

where $*$ denotes the conjugate transpose and D_A and D_L are diagonal matrices with the structure

$$D_A = \text{diag}\{\underbrace{1, \dots, 1}_r, \underbrace{\sigma_{r+1}^2, \dots, \sigma_{r+q}^2}_q, \underbrace{0, \dots, 0}_{n-r-q}\}, \quad D_L = \text{diag}\{\underbrace{0, \dots, 0}_r, \underbrace{\mu_{r+1}^2, \dots, \mu_{r+q}^2}_q, \underbrace{1, \dots, 1}_{n-r-q}\}. \quad (2.7)$$

Because the number of nonzero elements in all diagonalizations of A^*A and L^*L is equal to the ranks of A and L , respectively, we have

$$\begin{cases} r + q = \text{rank}(A), \\ n - r = \text{rank}(L), \end{cases} \implies \begin{cases} r = n - \text{rank}(L), \\ q = \text{rank}(A) + \text{rank}(L) - n. \end{cases} \quad (2.8)$$

We denote the columns of the matrices Y and U by $\{y_k\}_{k=1}^n$ and $\{u_k\}_{k=1}^m$, respectively. For simplicity, we shall drop the indices from the set notation $\{\cdot\}$ when referring to the entire set. The Fourier coefficients of the data with respect to the basis $\{u_k\}$ are denoted by $\beta_k \equiv u_k^* b$ and those of the noise by $\nu_k \equiv u_k^* n$. Using this notation and the decomposition (2.3), the Tikhonov solution can be written as

$$x_\lambda = \sum_{k=1}^r \beta_k y_k + \sum_{k=r+1}^{r+q} \frac{\gamma_k^2}{\gamma_k^2 + \lambda^2} \frac{\beta_k}{\sigma_k} y_k. \quad (2.9)$$

The first term in (2.9) is the projection of the regularized solution x_λ onto the nullspace of L spanned by vectors $\{y_k\}_{k=1}^r$ because the linearly independent vectors $\{y_k\}_{k=1}^r$, where $r = \dim \mathcal{N}(L)$, satisfy $Ly_k = 0$. Since the projection of the least squares solution of the unperturbed problem $Ax = b_{true}$ onto the null space $\mathcal{N}(L)$ is $\sum_{k=1}^r (\beta_k - \nu_k) y_k$, the first term in (2.9) contributes $\sum_{k=1}^r \nu_k y_k$ to the error in the regularized solution. Furthermore, this term is not filtered by Tikhonov regularization and is unaffected by the choice of λ , making this error irreducible. We must therefore require

$$\nu_k \ll \beta_k, \quad \text{for } k \leq r, \quad (2.10)$$

to keep this error small. The relation (2.10) holds in the vast majority of practical problems as $\{u_k\}_{k=1}^r$ are typically smooth vectors. Specifically, we have from (2.3) $Ay_k = u_k$ for $k \leq r$. Since the vectors $\{y_k\}_{k=1}^r$ are smooth (by assumption 2) and A has a typical smoothing effect [17, p. 21], $\{u_k\}_{k=1}^r$ are smooth as well. Therefore, only a small amount of noise is present in the first r terms in the expansion of the perturbed data in $\{u_k\}$ basis.

If L is nonsingular, the generalized singular values $\{\gamma_k\}$ are the regular singular values of AL^{-1} [17, sect. 2.1.2], [14]. In particular, if $L = I$ the SVD of A is given by

$$A = U \begin{pmatrix} S_A S_L^{-1} & \\ & O_A \end{pmatrix} V^*, \quad (2.11)$$

where $S_A S_L^{-1} = \text{diag}\{\gamma_1, \dots, \gamma_q\}$ and the matrices O_A , U and V are obtained from the GSVD (2.3). Furthermore, denoting the columns of V by $\{v_k\}$, it is easy to show that $y_j = \mu_j v_j$ for $j \leq \text{rank}(A)$ and $y_j = v_j$ for $j > \text{rank}(A)$. Thus, our expression for the Tikhonov solution (2.9) and the Fourier coefficients β_k and ν_k coincide with the ones given in [32, 25] when $L = I$.

We remark that our analysis is general enough to account for not only Tikhonov regularization, but also other forms of spectral filtering and particularly those in [32]. In fact, all the filters discussed in [32] can be implemented in our framework by simply substituting the generalized singular values $\{\gamma_k\}$ for the ordinary singular values of A into the definitions of the filters. Similarly, all our subsequent analysis and results can be easily generalized to arbitrary spectral filters.

3. Estimation of the regularization parameter.

3.1. The Series Splitting method. In this section we consider the problem of choosing a near-optimal value of the regularization parameter λ in (2.9). The discrete Picard condition (assumption 5) serves to guarantee the existence of such a value of λ corresponding to an accurate Tikhonov solution x_λ (see [13], [17, sect. 4.5], [32, sect. 2.1]). The discrete Picard condition implies

that the average decay of the sequence $\{|u_k^* b_{true}|\} = \{|\beta_k - \nu_k|\}$ towards zero is faster than that of $\{\gamma_k\}$, while according to assumption 4 we have $\gamma_k \approx 0$ from some $k = k_0$ on. Therefore, we have $|\beta_k - \nu_k| < \gamma_k \approx 0$ for all $k \geq k_0$. The index k_0 is called the Picard parameter and is used below.

We assess the quality of the solution x_λ by measuring the distance (1.4) between the unperturbed data $b - n$ and the data reconstructed from the Tikhonov solution

$$Ax_\lambda = \sum_{k=1}^r \beta_k u_k + \sum_{k=r+1}^{r+q} \frac{\gamma_k^2}{\gamma_k^2 + \lambda^2} \beta_k u_k. \quad (3.1)$$

We can rewrite (1.4) as

$$\begin{aligned} f(\lambda) &= \|n\|^2 + \|b - Ax_\lambda\|^2 - 2\Re[n^*(b - Ax_\lambda)] \\ &= \|n\|^2 + \rho(\lambda) - 2R(\lambda), \end{aligned} \quad (3.2)$$

where

$$\rho(\lambda) \equiv \|b - Ax_\lambda\|^2 = \sum_{k=r+1}^{r+q} \frac{\lambda^4}{(\gamma_k^2 + \lambda^2)^2} |\beta_k|^2 + \sum_{k=r+q+1}^m |\beta_k|^2, \quad (3.3)$$

is the squared residual norm,

$$R(\lambda) \equiv \Re[n^*(b - Ax_\lambda)] = \sum_{k=r+1}^{r+q} \frac{\lambda^2}{\gamma_k^2 + \lambda^2} \Re(\beta_k \cdot \overline{\nu_k}) + \sum_{k=r+q+1}^m \Re(\beta_k \cdot \overline{\nu_k}), \quad (3.4)$$

and $\Re(\cdot)$ denotes the real part.

The norm (1.4) is closely related to the predictive mean-square error (PMSE) defined in (1.5). Specifically, it is easy to show that

$$f(\lambda) - \text{PMSE}(\lambda) = \|b_{true}\|^2 - \|Ax_{true}\|^2, \quad (3.5)$$

and so, $f(\lambda)$ differs from the PMSE only by a constant that vanishes if A defines a consistent system so that $b_{true} = Ax_{true}$. Thus, we have $\lambda_{opt} = \arg \min f(\lambda) = \arg \min \text{PMSE}(\lambda)$.

Noting that the term $\|n\|^2$ in (3.2) is independent of λ and can therefore be neglected, we find that it is sufficient to minimize

$$g(\lambda) = \rho(\lambda) - 2R(\lambda). \quad (3.6)$$

A direct evaluation of (3.6) is not possible because the function $R(\lambda)$ depends on the unknown noise vector n . Nonetheless, we can accurately approximate $R(\lambda)$ using the Picard parameter [32, 25]. Recalling that the Picard parameter k_0 is the smallest index for which $u_k^* b_{true} = \beta_k - \nu_k \approx 0$ is satisfied for all $k \geq k_0$, we can split the sequence $\{\beta_k\}$ into two parts, the first part $\{\beta_k\}_{k=1}^{k_0-1}$, containing the information about the unperturbed data and the second part $\{\beta_k\}_{k=k_0}^m$ containing the noise. When $k < k_0$ the coefficients β_k and ν_k differ significantly, so we choose to approximate the term $\Re(\beta_k \cdot \overline{\nu_k})$ in (3.4) by replacing it with its expected value. Because of assumption 3, we have $\mathcal{E}(\Re(\beta_k \cdot \overline{\nu_k})) = \mathcal{E}(b_k n_k) = s^2$ where $\mathcal{E}(\cdot)$ denotes the expected value (see [19, sect. 6.6]). When

$k \geq k_0$, however, we have $\nu_k \approx \beta_k$ and so $\Re(\beta_k \cdot \overline{\nu_k}) \approx |\beta_k|^2$. Therefore, for given k_0 and s^2 we can evaluate $R(\lambda)$ by splitting the series (3.4) to obtain

$$R(\lambda) \approx s^2 \sum_{k=r+1}^{k_0-1} \frac{\lambda^2}{\gamma_k^2 + \lambda^2} + \sum_{k=k_0}^{r+q} \frac{\lambda^2}{\gamma_k^2 + \lambda^2} |\beta_k|^2 + \sum_{k=r+q+1}^m |\beta_k|^2. \quad (3.7)$$

The approximate λ_{opt} can be found by minimizing (3.6) with $R(\lambda)$ given by (3.7). The algorithm for the SS method described in subsection 3.1 is presented in Algorithm 3.

We can limit k_0 to the interval $[r+1, r+q]$ by considering the largest index below which the signal must dominate the noise, and a sufficiently large one for which $\beta_k - \nu_k \approx 0$ is guaranteed to hold. To justify the lower bound $k_0 \geq r+1$, we recall from section 2 that for $k_0 < r+1$ we have $\nu_k \ll \beta_k$ because the vectors $\{u_k\}_{k=1}^r$ are smooth. Therefore, $\beta_k - \nu_k \not\approx 0$ for $k \leq r$ and so, $k_0 \geq r+1$. To justify the upper-bound, we note that γ_{r+q} is the last numerically nonzero generalized singular value of A and so by assumption 4, $\gamma_{r+q} \approx \epsilon$ where ϵ is the machine zero. Thus, by the discrete Picard condition, $\beta_{r+q} - \nu_{r+q} \approx 0$ and we can conclude that $k_0 \leq r+q$. If $L = I$ as in [32, 25], we have $r = 0$ and only the upper-bound $k_0 \leq \text{rank}(A)$ is nontrivial. We conclude from the above arguments that we can always split the sums in (3.4).

3.2. Estimating the Picard parameter and the variance of the noise. We begin with a brief discussion of the methods for estimation of the Picard parameter suggested in [32]. The Picard parameter can be found graphically from the plot of the sequence $\{\beta_k\}$ versus k . Specifically, because of the discrete Picard condition, the plot of $\{\beta_k\}$ is expected to decay on average with increasing index and level off at the Picard parameter. This levelling off can be found manually from the plot, see [32, sect. 2.2]. In [32, sect. 2.3] it is suggested to use the Lilliefors test for normality on subsequences of $\{\beta_k\}$ in order to automate the graphical estimation of the Picard parameter. Specifically, this method sets k_0 to the smallest index for which the sequence $\{\beta_k\}_{k=k_0}^m$ is dominated by Gaussian noise. By applying the Lilliefors test at 95% confidence to the sequences $\{\beta_k\}_{k=j}^m$ for $j = m-3, m-2, \dots, 1$, the Picard parameter k_0 is chosen to be the smallest index after which the test fails 10 consecutive times. If the test fails immediately, at $j = m-3$, it is proposed to set $k_0 = m+1$ and $s^2 = 0$, signifying that the data is noiseless. Alternative tests that assume different distributions can be utilized in a similar way if the noise is not Gaussian [32]. Once k_0 is found, the variance s^2 can be estimated as the sample variance of the sequence $\{\beta_k\}_{k=k_0}^m$ using the expression

$$s^2 \approx \frac{1}{m - k_0 + 1} \sum_{k=k_0}^m |\beta_k - \bar{\beta}|^2, \quad (3.8)$$

where

$$\bar{\beta} = \frac{1}{m - k_0 + 1} \sum_{j=k_0}^m \beta_j, \quad (3.9)$$

is the sample mean.

We find that one can improve the accuracy of the method described above by initializing the estimate of k_0 to its lower bound $r+1$ and applying the Lilliefors test to the sequences $\{\beta_k\}_{k=j}^m$ for

$j = r + 1, r + 2, \dots, r + q$ at the 99.9% confidence level. The value of k_0 is set to the smallest index j for which the Lilliefors test indicates that the sequence is normally distributed. If the test fails for $j = r + q$, we set $k_0 = r + q$ and $s^2 = 0$. Once k_0 is estimated, we can find the variance using (3.8). The modified algorithm is summarized in Algorithm 2. In contrast to the algorithm in [32], which gives inaccurate results for some noise realizations, the modified algorithm is accurate in all numerical example, but still depends on the assumed distribution of the noise.

The dependence of the method for estimation of the Picard parameter on statistical tests can be avoided using a new method which is based on the following idea. The expected value of the squared moduli of the Fourier coefficients β_k is given by

$$\mathcal{E}(|\beta_k|^2) = \begin{cases} |\beta_k - \nu_k|^2 + s^2 & \text{if } k < k_0, \\ s^2 & \text{if } k \geq k_0, \end{cases} \quad (3.10)$$

where we use the fact that $\beta_k - \nu_k \approx 0$ for $k \geq k_0$. If the discrete Picard condition is satisfied, the sequence $\{|\beta_k - \nu_k|^2\}$ decreases on average with increasing k up to $k = k_0$. Thus, if we could compute (3.10) in practice, we would simultaneously find both k_0 and s^2 by detecting the levelling off of $\{\mathcal{E}(|\beta_k|^2)\}$. However, even though $\{\mathcal{E}(|\beta_k|^2)\}$ is not known, it is possible to approximate the expected value (3.10) for $k \geq k_0$ by the average

$$V(k) \equiv \frac{1}{m - k + 1} \sum_{j=k}^m |\beta_j|^2. \quad (3.11)$$

Assuming that m is sufficiently large, (3.11) represents a good approximation to (3.10) for $k \geq k_0$. We note, however, that if $k \approx m$, the expression (3.11) ceases to be a good approximation to the expected value (3.10) because of the small number of terms in (3.11).

For $k < k_0$, (3.11) can be rewritten as

$$V(k) \approx s^2 + \frac{1}{m - k + 1} \sum_{j=k}^{k_0-1} |\beta_j - \nu_j|^2 \quad \forall k < k_0, \quad (3.12)$$

and since the last term in (3.12) is a sum of positive quantities,

$$V(k_2) > V(k_1) \quad \forall k_1 \geq k_0 > k_2. \quad (3.13)$$

Therefore, the sequence $\{V(k)\}_{k=r+1}^{r+q}$ decreases until it levels at s^2 when $k = k_0$, similarly to the expected value (3.10).

Using the arguments above, we can estimate the Picard parameter by setting $k = r + 1$ and then increasing k until the condition

$$\frac{|V(k+1) - V(k)|}{V(k+1)} < \varepsilon, \quad (3.14)$$

is satisfied for two consecutive values of k and for some small $\varepsilon > 0$. The value of ε has to be small enough to detect the levelling off of $V(k)$ but large enough to account for its small, but nonzero, variance. Once k_0 is found, we can estimate the variance as $s^2 \approx V(k_0)$. If $V(k)$ does not satisfy (3.14) for any $r + 1 \leq k_0 \leq r + q$, we assume the data to be noiseless and set $k_0 = r + q$ and $s^2 = 0$.

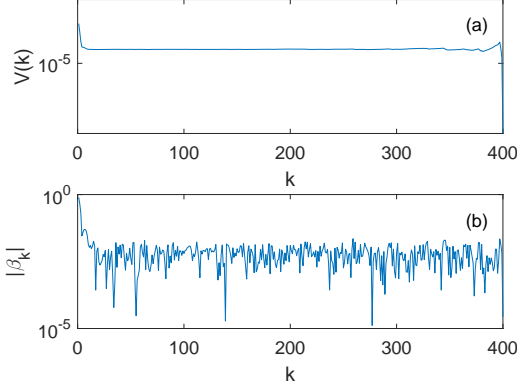


Figure 3.1: Comparison of (a) $\log V(k)$ and (b) $\log \beta_k$ for the test problem `heat` from [16], corrupted with white Gaussian noise with $s^2 / \max\{|b_{true;k}|^2\} = 10^{-2}$. Here, we use $L = I$ as in [32]. The non-negligible fluctuations of β_k in (b) and in contrast, almost smooth $V(k)$ in (a) are clearly seen.

Figure 3.1 clearly illustrates the difference between the graphical method in [32] for estimation of the Picard parameter and the new method, presented above. Even though each method is based on detection of the levelling off of a sequence, $\{\beta_k\}$ for the graphical method or $\{V(k)\}$ for the new method, the plot of $\{V(k)\}$ shown in Figure 3.1(a) remains almost constant for $k \geq k_0$, whereas $\{\beta_k\}$ shown in Figure 3.1(b) oscillates with a non-negligible variance. Because of the oscillations, the exact point at which the plot of $\{\beta_k\}$ levels off cannot be unambiguously determined. In contrast, $V(k)$ in Figure 3.1(a) flattens almost completely from $k = k_0$ up to $k \approx 380$, where it ceases to be a good approximation to (3.10). We summarize the procedure in Algorithm 1.

Algorithm 1 Estimating the Picard parameter using the sequence $\{V(k)\}_{k=r+1}^{k=r+q}$

Input: $\{\beta_k\}, r, q, \varepsilon$

Output: k_0, s^2

```

 $k_0 \leftarrow r + 1$  ▷ Initialize the Picard parameter  $k_0$  to its lower bound
 $V(k) = \left( \sum_{j=k}^m |\beta_j|^2 \right) / (m - k + 1)$  ▷ Define  $V(k)$  as in (3.11)
while  $(|V(k_0+1) - V(k_0)| / V(k_0+1) \geq \varepsilon$  or  $|V(k_0+2) - V(k_0+1)| / V(k_0+2) \geq \varepsilon)$  and  $k_0 < r + q + 1$ 
do
     $k_0 \leftarrow k_0 + 1$  ▷ Increase  $k_0$  as long as the condition (3.14) is not satisfied and  $k_0$  is below
▷ the upper bound
end while
if  $k_0 = r + q + 1$  then ▷ Check whether  $k_0$  exceeds the upper bound
     $s^2 \leftarrow 0$  ▷ If yes, data is noiseless
     $k_0 \leftarrow r + q$ 
else
     $s^2 \leftarrow V(k_0)$  ▷ Otherwise estimate the variance  $s^2$  as  $V(k_0)$ 
end if

```

3.3. The Data Filtering approach. In this section we describe the DF method which generalizes the SS method for minimization of (1.4). The DF method uses the Picard parameter to directly approximate the clean data $b - n$, instead of approximating the noise-dependent terms in (1.4) as done in subsection 3.1. We assume that the sequence $\{\beta_k\}_{k=1}^{k_0-1}$ has negligible noise and can be regarded as the true data in basis $\{u_k\}$, while the sequence $\{\beta_k\}_{k=k_0}^m$ is dominated by noise. To

Algorithm 2 Estimating the Picard parameter using the Lilliefors test**Input:** $\{\beta_k\}, r, q$ **Output:** k_0, s^2

```

 $k_0 \leftarrow r + 1$  ▷ Initialize the Picard parameter  $k_0$  to its lower bound
while  $\text{lilliefors}(\{\beta_k\}_{k=k_0}^m, .999) \neq 0$  and  $k_0 < r + q + 1$  do
  ▷  $\text{lilliefors}(\{\cdot\}, .999)$  returns 1 if the Lilliefors test rejects the null hypothesis at 99.9%
  ▷ confidence level and 0 otherwise
   $k_0 \leftarrow k_0 + 1$ 
end while
if  $k_0 = r + q + 1$  then ▷ Check whether  $k_0$  exceeds the upper bound
   $s^2 \leftarrow 0$  ▷ If yes, data is noiseless
   $k_0 \leftarrow r + q$ 
else
   $s^2 \leftarrow (\sum_{k=k_0}^m |\beta_k|^2) / (m - k_0 + 1)$  ▷ Otherwise estimate the variance  $s^2$  as in (3.8) with  $\bar{\beta} = 0$ 
end if

```

Algorithm 3 The SS method**Input:** A, L, b, ε **Output:** x_{SS}

```

 $[m, n] \leftarrow \text{size}(A)$  ▷ size = [no. of rows, no. of columns]
 $r \leftarrow n - \text{rank}(L)$ 
 $q \leftarrow \text{rank}(A) + \text{rank}(L) - n$ 
 $[\{\sigma_k\}, \{\mu_k\}, \{y_k\}, \{u_k\}] \leftarrow \text{GSVD}(A, L)$  ▷ Perform GSVD of the pair  $(A, L)$ 
 $\{\gamma_k\} \leftarrow \{\sigma_k / \mu_k\}$  ▷ Define the generalized singular values
 $\{\beta_k\} \leftarrow \{u_k^* b\}$  ▷ Define the Fourier coefficients of  $b$  with respect to  $\{u_k\}$ 
 $x(\lambda) = \sum_{k=1}^r \beta_k y_k + \sum_{k=r+1}^{r+q} \frac{\gamma_k^2}{\gamma_k^2 + \lambda^2} \frac{\beta_k}{\sigma_k} y_k$  ▷ Define the Tikhonov solution as in (2.9)
 $\rho(\lambda) = \|b - Ax(\lambda)\|^2$  ▷ Define  $\rho(\lambda)$  as in (3.3)
 $[k_0, s^2] \leftarrow \text{Algorithm 1}(\{\beta_k\}, r, q, \varepsilon)$  ▷ Get  $k_0$  and  $s^2$  from Algorithm 1
 $R(\lambda) = s^2 \sum_{k=r+1}^{k_0-1} \frac{\lambda^2}{\gamma_k^2 + \lambda^2} + \sum_{k=k_0}^{r+q} \frac{\lambda^2}{\gamma_k^2 + \lambda^2} |\beta_k|^2 + \sum_{k=r+q+1}^m |\beta_k|^2$  ▷ Define  $R(\lambda)$  as in (3.4)
 $g(\lambda) = \rho(\lambda) - 2R(\lambda)$  ▷ Define the function to be minimized as in (3.6)
 $\lambda_{found} \leftarrow \arg \min_{\lambda \in [0, \infty)} g(\lambda)$  ▷ Find  $\lambda \geq 0$  minimizing  $g(\lambda)$ 
 $x_{SS} \leftarrow x(\lambda_{found})$ 

```

approximate $b - n$, we form the vector

$$\hat{\beta} = (u_1^* b, \dots, u_{k_0-1}^* b, \underbrace{0, \dots, 0}_{m-k_0+1})^T$$

and transform it back to the standard basis

$$b - n \approx \hat{b} = U \hat{\beta} = \sum_{k=1}^{k_0-1} \beta_k u_k. \quad (3.15)$$

In the DF method we minimize the norm $\hat{f}(\lambda) = \|\hat{b} - Ax_\lambda\|$ instead of working with $f(\lambda)$ defined in (1.4). Since the true data is usually smooth because of the typical smoothing effect of A on x_{true} [17, p. 21], this data filter is unlikely to remove parts of the true data along with the noise. Note that the DF method can be generalized to use different data filters and regularization methods. All it requires is an accurate data filter and an algorithm for producing a regularized solution given some regularization parameter. The DF method is summarize in Algorithm 4.

Algorithm 4 The DF method

Input: A, L, b, ε

Output: x_{DFA}

$[m, n] \leftarrow \text{size}(A)$ $r \leftarrow n - \text{rank}(L)$ $q \leftarrow \text{rank}(A) + \text{rank}(L) - n$ $[\{\sigma_k\}, \{\mu_k\}, \{y_k\}, \{u_k\}] \leftarrow \text{GSVD}(A, L)$ $\{\gamma_k\} \leftarrow \{\sigma_k / \mu_k\}$ $\{\beta_k\} \leftarrow \{u_k^* b\}$ $k_0 \leftarrow \text{Algorithm 1}(\{\beta_k\}, r, q, \varepsilon)$ $\hat{b} \leftarrow \sum_{k=1}^{k_0-1} \beta_k u_k$ $x(\lambda) = \sum_{k=1}^r \beta_k y_k + \sum_{k=r+1}^{r+q} \frac{\gamma_k^2}{\gamma_k^2 + \lambda^2} \frac{\beta_k}{\sigma_k} y_k$ $\hat{f}(\lambda) = \ \hat{b} - Ax(\lambda)\ ^2$ $\lambda_{found} \leftarrow \arg \min_{\lambda \in [0, \infty)} \hat{f}(\lambda)$ $x_{DFA} \leftarrow x(\lambda_{found})$	$\triangleright \text{size} = [\text{no. of rows}, \text{no. of columns}]$ $\triangleright \text{Perform GSVD of } (A, L)$ $\triangleright \text{Define the generalized singular values}$ $\triangleright \text{Define the Fourier coefficients of } b \text{ with respect to } \{u_k\}$ $\triangleright \text{Get } k_0 \text{ from Algorithm 1}$ $\triangleright \text{Get filtered data as in (3.15)}$ $\triangleright \text{Define Tikhonov solution as in (2.9)}$ $\triangleright \text{Define the function to be minimized}$ $\triangleright \text{Find } \lambda \geq 0 \text{ minimizing } \hat{f}(\lambda)$
----------------------------------------------------------------------------------------------------------------------------------------------------------------------------------------------------------------------------------------------------------------------------------------------------------------------------------------------------------------------------------------------------------------------------------------------------------------------------------------------------------------------------------------------------------------------------------------------------------------------------------------------------------------------------------------------------------------------------------------------------------------	--------------------------------------------------------------------------------------------------------------------------------------------------------------------------------------------------------------------------------------------------------------------------------------------------------------------------------------------------------------------------------------------------------------------------------------------------------------------------------------------------------------------------------------------------------------------------------------------------------------------------------------------------

4. Relation to other methods. In this section we describe the relationship between the SS, SURE and the GCV methods. In particular, we show that similarly to the SS method, the SURE and the GCV methods minimize an approximation of $f(\lambda)$ in (1.4). As discussed in section 3, the SS method approximates (1.4) by using the Picard parameter to split the sum $R(\lambda)$ and by taking the expected value of only a part of the sum as written in (3.7). In contrast, the SURE method approximates $f(\lambda)$ by taking the expected value of $\|n\|^2$ and of the whole $R(\lambda)$ without splitting it. The SURE method thus minimizes the function

$$\text{SURE}(\lambda) = \rho(\lambda) + ms^2 - 2s^2 T(\lambda), \quad (4.1)$$

where

$$T(\lambda) = \frac{\mathcal{E}(R(\lambda))}{s^2} = m - \text{rank}(A) + \sum_{k=r+1}^{r+q} \frac{\lambda^2}{\gamma_k^2 + \lambda^2}, \quad (4.2)$$

Therefore the SS method approximates $R(\lambda)$ better because the sum containing $|\beta_k|^2$ in (3.7) capture at least part of the true, oscillatory behavior of $\Re(\beta_k \cdot \overline{v_k})$, in contrast to the SURE method which replaces the whole term with a constant.

Another popular method for determining λ is the Generalized Cross-Validation (GCV) [37, 10], which relies on the minimization of the function

$$G(\lambda) = \frac{\rho(\lambda)}{(T(\lambda))^2}. \quad (4.3)$$

In spite of the different forms of the SURE and GCV functions it can be shown that their minima are close to each other. Specifically, it is easy to show that

$$T(\lambda) = \text{trace}(I - H_\lambda), \quad (4.4)$$

where $H_\lambda = A(A^*A + \lambda^2 L^*L)^{-1}A^*$. The quantity $T(\lambda)$ is equivalent to the residual effective degrees of freedom in regression, see [37, p. 63]. Therefore, the following approximation holds in an interval containing the minimum of (4.3)

$$\frac{\rho(\lambda)}{T(\lambda)} \approx s^2, \quad (4.5)$$

see [37, sect. 4.7], [14, sect. 6.3]. Using the approximation (4.5) we see that the local minima of both $\text{SURE}(\lambda)$ in (4.1) and $G(\lambda)$ in (4.3) satisfy

$$\rho'(\lambda^*) = 2s^2T'(\lambda^*), \text{ and } \rho''(\lambda^*) - 2s^2T''(\lambda^*) > 0, \quad (4.6)$$

where λ^* is the argument of the minimum of either function. Even though the local minima of the methods are similar, their global minima may differ. This result implies that both the SURE method and the GCV method rely on replacing $R(\lambda)$ in (3.4) with its expected value $s^2T(\lambda)$ in (4.2). Thus, they both rely on an inferior approximation of $R(\lambda)$ compared with our SS method as explained above. For additional analysis of the relation between the SURE method and the GCV method, see [23].

5. Numerical examples. In this section we present the results of the numerical simulations. The performance of the new methods is compared to that of the SURE method and the GCV method on three test problems from the **Regularization Tools** package [16]: the one-dimensional gravity-surveying problem **gravity**, Phillips' test problem from [28] **phillips**, and the inverse heat equation **heat**. We use three different algorithms to estimate the Picard parameter and the variance of the noise for the SS method - our Algorithm 1 with $\varepsilon = 3 \times 10^{-2}$ (denoted SS+P), the algorithm that uses the Lilliefors test proposed in [32, sect. 2.3] (denoted SS+OL) and its modified version described in Algorithm 2 (denoted SS+ML). For SS+OL, we use the **Matlab** code provided in [32, sect. 6]. We note that this algorithm occasionally gives a Picard parameter outside the interval $r+1 \leq k_0 \leq r+q$. In this case, if $k_0 > r+q$, the second sum in (3.7) vanishes and the lower bound on the first sum becomes $r+1$, whereas if $k_0 < r+1$ the first sum vanishes and the upper bound on the second sum becomes $r+q$. For the implementations of the DF method and the SURE method we use only our Algorithm 1 to estimate the Picard parameter and noise variance.

For each problem, we generate a 400×400 coefficient matrix A along with the true solution vector x_{true} and the unperturbed data vector b_{true} . We use **Matlab**'s **randn** function to add white Gaussian noise of zero mean and a variance of $s^2 = \alpha \max\{|b_{true}|^2\}$, where $\alpha \in \{10^{-2}, 10^{-3}, 10^{-4}\}$. We thus present a total of nine tests and for each test we generate 1000 independent noise realizations. We choose L to be $D^{(m)}$, the finite difference approximation to the m th derivative. Then, we set

- For **gravity** problem: $L = D^{(1)}$ with $\text{rank}(L) = 399$ and $\text{rank}(A) = 46$.
- For **phillips** problem: $L = D^{(2)}$ with $\text{rank}(L) = 398$, $\text{rank}(A) = 400$ and $\text{cond}(A) = 6.77 \times 10^8$.

- For **heat** problem: $L = I$ with $\text{rank}(L) = 400$ and $\text{rank}(A) = 393$.

To assess the performance of each method, we use the mean-square deviation (MSD) defined as

$$\text{MSD}(\lambda) = \frac{\|x_{true} - x_\lambda\|^2}{\|x_{true}\|^2}. \quad (5.1)$$

The optimal solution is then defined as the one minimizing the MSD (5.1). If a method produces an MSD value larger than $1/2$ for a given noise realization, we consider it a failure of the method since such a solution has a relative error of over 50%.

5.1. Results. In Figure 5.1-Figure 5.9, we present the results of our simulations by means of boxplots of the MSD values in log scale. Boxplots graphically depict the results by splitting them into quartiles so that each box spans the interval between the first quartile and the third quartile, called the interquartile range (i.e., the middle 50% of the data). The horizontal line in each box denotes the median and the error bars span 150% of the interquartile range above the third quartile and below the first quartile. Any point outside this interval is considered an outlier and is denoted by '+'. Note that the outliers, as they are defined here, are used only for visualization purposes, and therefore do not utilize an absolute cutoff, while the definition of the failures sets a rigid cutoff above which solutions are useless. The large number of outliers produced by the GCV, SURE and SS+OL methods, shown in Figure 5.1-Figure 5.9 is consistent with the failure rates presented in Table 5.1 (only methods with nonzero failure rate are shown in the table).

The inability of the SS+OL method to find an acceptable value of λ in a non-negligible percentage of noise realizations is caused by poor estimation of the Picard parameter. On the other hand, both Algorithm 1 and Algorithm 2 perform well as is demonstrated by the numerical results. In addition, Algorithm 1 used by SS+P is superior to Algorithm 2 used by SS+ML in the vast majority of the examples. While their performance is quite similar, the median of SS+P is usually slightly lower than that of SS+ML. The difference between the results of SS+P and the DF method, however, is negligible, implying that there is no significant difference between approximation of the noise dependent terms in SS+P and approximation of the noiseless data in the DF method. Finally, it should be noted that the median MSD values of the GCV, SURE and SS+OL methods are relatively close to those of the SS+P and the DF methods in spite of the high failure rate of the former.

REFERENCES

- [1] FRANK BAUER AND STEFAN KINDERMANN, *The quasi-optimality criterion for classical inverse problems*, Inverse Problems, 24 (2008), p. 035002.
- [2] FRANK BAUER, MARKUS REISS, AND MARKUS REISS, *Regularization independent of the noise level: an analysis of quasi-optimality*, Inverse Problems, 24 (2007), p. 18.
- [3] MIKHAIL BELKIN, PARTHA NIYOGI, AND VIKAS SINDHWANI, *Manifold regularization: A geometric framework for learning from labeled and unlabeled examples*, Journal of Machine Learning Research, 7 (2006), pp. 2399–2434.
- [4] J. BIEMOND, R.L. LAGENDIJK, AND R.M. MERSEREAU, *Iterative methods for image deblurring*, Proceedings of the IEEE, 78 (1990), pp. 856–883.
- [5] DAVID COLTON AND RAINER KRESS, *Integral Equation Methods in Scattering Theory*, Society for Industrial and Applied Mathematics (SIAM), 2013.

- [6] JANE CULLUM, *The Effective Choice of the Smoothing Norm in Regularization*, Mathematics of Computation, 33 (1979), pp. 149–170.
- [7] WEISHENG DONG, LEI ZHANG, GUANGMING SHI, AND XIAOLIN WU, *Image deblurring and super-resolution by adaptive sparse domain selection and adaptive regularization.*, IEEE transactions on image processing : a publication of the IEEE Signal Processing Society, 20 (2011), pp. 1838–57.
- [8] N P GALATSANOS AND A K KATSAGGELOS, *Methods for choosing the regularization parameter and estimating the noise variance in image restoration and their relation.*, IEEE transactions on image processing : a publication of the IEEE Signal Processing Society, 1 (1992), pp. 322–36.
- [9] GENE H. GOLUB, PER CHRISTIAN HANSEN, AND DIANNE P. O’LEARY, *Tikhonov Regularization and Total Least Squares*, SIAM Journal on Matrix Analysis and Applications, 21 (1999), pp. 185–194.
- [10] GENE H GOLUB, MICHAEL HEATH, AND GRACE WAHBA, *Generalized cross-validation as a method for choosing a good ridge parameter*, Technometrics, 21 (1979), pp. 215–223.
- [11] WOLFGANG HACKBUSCH, *Integral Equations*, Birkhäuser Basel, Basel, 1995.
- [12] PER CHRISTIAN HANSEN, *Regularization, GSVD and truncated GSVD*, BIT, 29 (1989), pp. 491–504.
- [13] ———, *The discrete picard condition for discrete ill-posed problems*, Bit, 30 (1990), pp. 658–672.
- [14] ———, *Analysis of Discrete Ill-Posed Problems by Means of the L-Curve*, SIAM Review, 34 (1992), pp. pp. 561–580.
- [15] P C HANSEN, *Numerical tools for analysis and solution of Fredholm integral equations of the first kind*, 1992.
- [16] PER CHRISTIAN HANSEN, *REGULARIZATION TOOLS: A Matlab package for analysis and solution of discrete ill-posed problems*, Numerical Algorithms, 6 (1994), pp. 1–35.
- [17] ———, *Rank-Deficient and Discrete Ill-Posed Problems*, Society for Industrial and Applied Mathematics, 1998.
- [18] ———, *Discrete Inverse Problems*, Society for Industrial and Applied Mathematics, 2010.
- [19] PER CHRISTIAN HANSEN, JAMES G. NAGY, AND DIANNE P. O’LEARY, *Deblurring Images*, Society for Industrial and Applied Mathematics (SIAM), 2006.
- [20] PER CHRISTIAN HANSEN AND DIANNE PROST O’LEARY, *The Use of the L-Curve in the Regularization of Discrete Ill-Posed Problems*, SIAM Journal on Scientific Computing, 14 (1993), pp. 1487–1503.
- [21] MISHA E. KILMER, PER CHRISTIAN HANSEN, AND MALENA I. ESPAÑOL, *A Projection-Based Approach to General-Form Tikhonov Regularization*, SIAM Journal on Scientific Computing, 29 (2007), pp. 315–330.
- [22] RAINER KRESS, *Linear Integral Equations*, vol. 82 of Applied Mathematical Sciences, Springer New York, New York, NY, 2014.
- [23] KER-CHAU LI, *From Stein’s Unbiased Risk Estimates to the Method of Generalized Cross Validation*, The Annals of Statistics, 13 (1985), pp. 1352–1377.
- [24] RUSSELL M. MERSEREAU, *Optimal estimation of the regularization parameter and stabilizing functional for regularized image restoration*, Optical Engineering, 29 (1990), p. 446.
- [25] DIANNE P. O’LEARY, *Near-Optimal Parameters for Tikhonov and Other Regularization Methods*, SIAM Journal on Scientific Computing, 23 (2001), pp. 1161–1171.
- [26] JOÃO P. OLIVEIRA, JOSÉ M. BIOUCAS-DIAS, AND MÁRIO A.T. FIGUEIREDO, *Adaptive total variation image deblurring: A majorizationminimization approach*, Signal Processing, 89 (2009), pp. 1683–1693.
- [27] C. C. PAIGE AND M. A. SAUNDERS, *Towards a Generalized Singular Value Decomposition*, SIAM Journal on Numerical Analysis, 18 (1981), pp. 398–405.
- [28] DAVID L. PHILLIPS, *A Technique for the Numerical Solution of Certain Integral Equations of the First Kind*, Journal of the ACM, 9 (1962), pp. 84–97.
- [29] SATHISH RAMANI, THIERRY BLU, AND MICHAEL UNSER, *Monte-Carlo sure: A black-box optimization of regularization parameters for general denoising algorithms*, IEEE Transactions on Image Processing, 17 (2008), pp. 1540–1554.
- [30] ALEX J. SMOLA, BERNHARD SCHÖLKOPF, BERNHARD SCH, AND BERNHARD SCHÖLKOPF, *A Tutorial on Support Vector Regression*, Statistics and Computing, 14 (2004), pp. 199–222.
- [31] CHARLES M. STEIN, *Estimation of the Mean of a Multivariate Normal Distribution*, The Annals of Statistics, 9 (1981), pp. 1135–1151.
- [32] VIKTORIA TAROUDAKI AND DIANNE P. O’LEARY, *Near-Optimal Spectral Filtering and Error Estimation for Solving Ill-Posed Problems*, SIAM Journal on Scientific Computing, 37 (2015), pp. A2947–A2968.
- [33] A. N. TIKHONOV AND V. Y. ARSENNIN, *Solutions of Ill-Posed Problems*, Mathematics of Computation, 32 (1978), pp. 1320–1322.
- [34] S. TWOMEY, *On the Numerical Solution of Fredholm Integral Equations of the First Kind by the Inversion of the Linear System Produced by Quadrature*, Journal of the ACM, 10 (1963).

- [35] V N VAPNIK, *The Nature of Statistical Learning Theory*, vol. 8, 1995.
- [36] FERMÍN S VILOCHE BAZÁN AND JULIANO B FRANCISCO, *An improved fixed-point algorithm for determining a Tikhonov regularization parameter*, *Inverse Problems*, 25 (2009), p. 045007.
- [37] GRACE WAHBA, *Spline Models for Observational Data*, Society for Industrial and Applied Mathematics (SIAM), 1990.
- [38] G. WAHBA AND Y. WANG, *When is the optimal regularization parameter insensitive to the choice of the loss function ?*, *Communications in Statistics - Theory and Methods*, 19 (1990), pp. 1685–1700.
- [39] CHRISTOPHER K. I WILLIAMS, *Learning With Kernels: Support Vector Machines, Regularization, Optimization, and Beyond*, *Journal of the American Statistical Association*, 98 (2003), pp. 489–489.
- [40] LU YUAN, JIAN SUN, LONG QUAN, AND HEUNG-YEUNG SHUM, *Image deblurring with blurred/noisy image pairs*, *ACM Transactions on Graphics*, 26 (2007), p. 1.
- [41] TONG ZHANG, *An Introduction to Support Vector Machines and Other Kernel-Based Learning Methods*, *AI Magazine*, 22 (2001), p. 103.

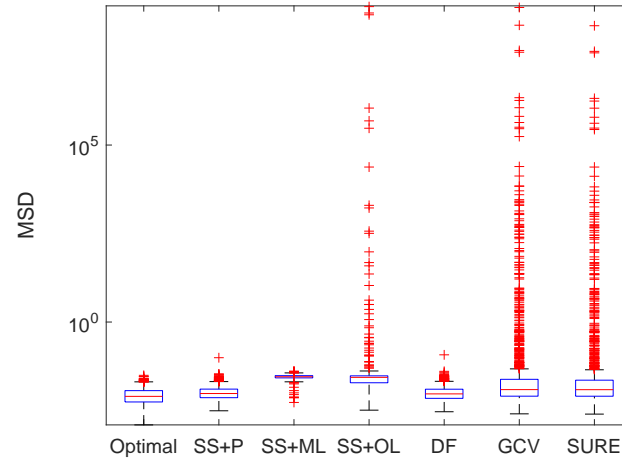


Figure 5.1: MSD values in log scale for **gravity** example, $L = D^{(1)}$, $\alpha = 10^{-2}$

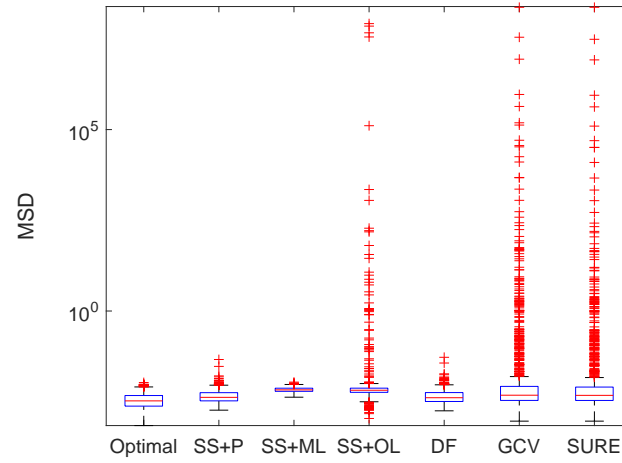


Figure 5.2: MSD values in log scale for **gravity** example, $L = D^{(1)}$, $\alpha = 10^{-3}$

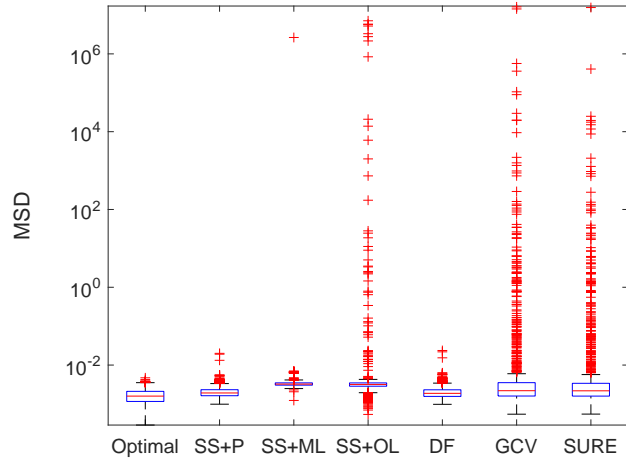


Figure 5.3: MSD values in log scale for **gravity** example, $L = D^{(1)}$, $\alpha = 10^{-4}$

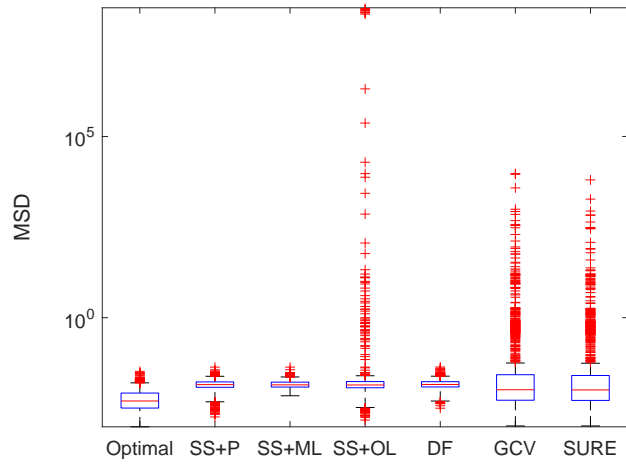


Figure 5.4: MSD values in log scale for **phillips** example, $L = D^{(2)}$, $\alpha = 10^{-2}$

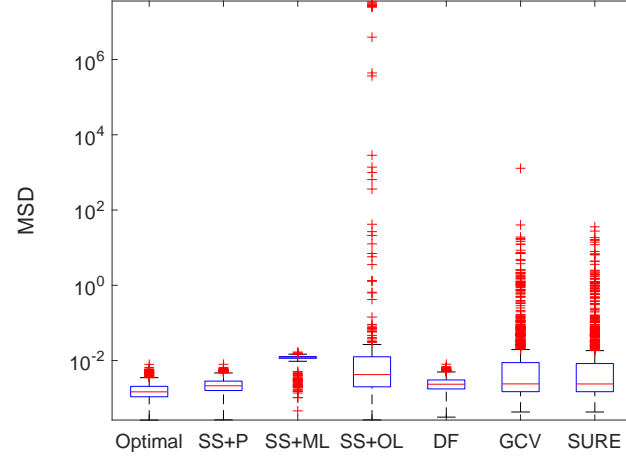


Figure 5.5: MSD values in log scale for **phillips** example, $L = D^{(2)}$, $\alpha = 10^{-3}$

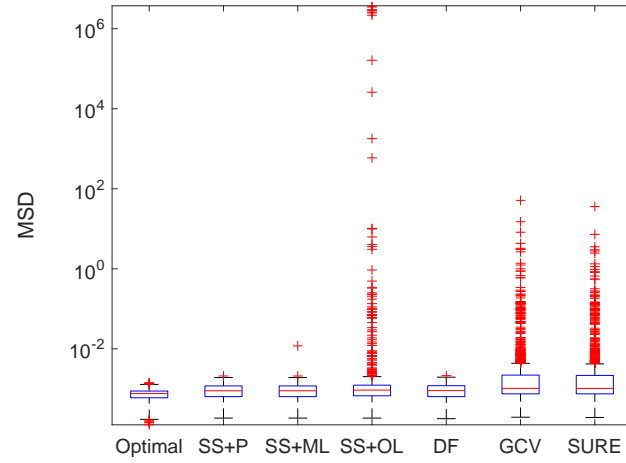
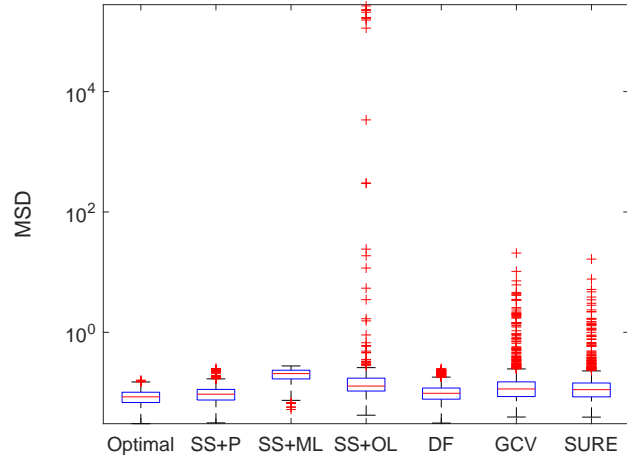
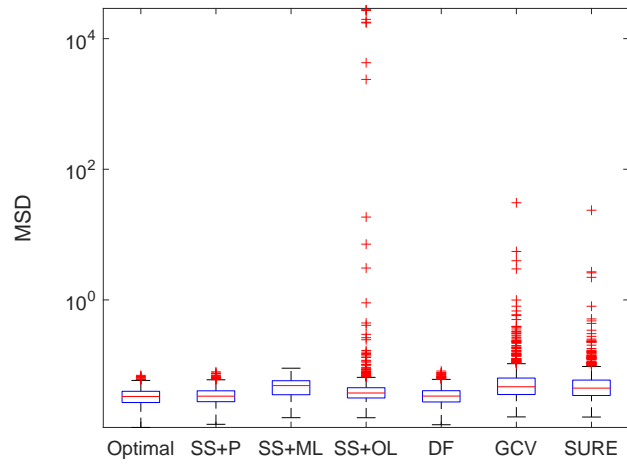


Figure 5.6: MSD values in log scale for **phillips** example, $L = D^{(2)}$, $\alpha = 10^{-4}$

Figure 5.7: MSD values in log scale for `heat` example, $L = I$, $\alpha = 10^{-2}$ Figure 5.8: MSD values in log scale for `heat` example, $L = I$, $\alpha = 10^{-3}$

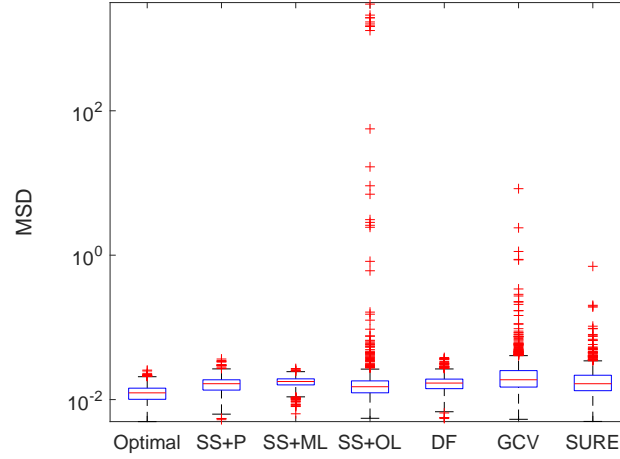


Figure 5.9: MSD values in log scale for **heat** example, $L = I$, $\alpha = 10^{-4}$

Table 5.1: Failure rates for the SS+ML, SS+OL, GCV and SURE methods for each of the three test problems and three noise levels. The SS+P and DF methods did not fail in our tests. The failure rate is defined as the fraction of the solutions with MSD values larger than $1/2$ for each test problem.

α	gravity			phillips			heat		
	1e-2	1e-3	1e-4	1e-2	1e-3	1e-4	1e-2	1e-3	1e-4
SS+ML	0%	0%	0.1%	0%	0%	0%	0%	0%	0%
SS+OL	2.4%	2.8%	2.9%	4.9%	2.9%	1.9%	2.2%	1.2%	1.9%
GCV	10.8%	8.1%	7.2%	13.6%	5.5%	1.6%	5.4%	1.0%	0.5%
SURE	10.1%	7.2%	6.5%	12.6%	5.2%	1.4%	4.0%	0.6%	0.1%